EXPERIMENTAL CHARACTERIZATION AND DAMAGE MODEL OF THE HUMAN SKIN RESPONSE TO DYNAMIC LOADINGS

JACQUEMOUD Clémentine[1,2], CORET Michel[2], BRUYÈRE-GARNIER Karine[1], BRUNET Michel[2]

[1]Laboratoire de Biomécanique et Mécanique des Chocs – UMR_T 9406 – INRETS/UCBL1
[2]Laboratoire de Mécanique des Contacts et des Structures – CNRS UMR5259 - INSA-Lyon

ABSTRACT

The objective of this work is to characterize and to model the damage of planar and fibrous soft tissues at high strain rate. As first step, we choose to study the human skin.
A dynamic tensile test up to failure is performed on 10x30mm human skin samples. The test is based on the drop test principle and allows loading of samples at a strain rate close to 40 s^{-1}. Classical measurement techniques give global strains whereas a full local strain field is measured on the sample surface by an Image Correlation Method (Mguil – Touchal, 1998). The behavior of the skin is simulated using a collagen fiber network defined by an angular distribution of fibers as proposed by Billiar and Sacks (2000). This model is extended to the damage phase by using a brittle hyper elastic behavior for the fibers.
The skin seems stiffer in the transverse direction than in the cranio-caudal direction and the strain field measurements show the heterogeneity of the tissue.
First, the model parameters are identified on a representative experimental curve obtained for the human forehead skin in the transverse direction. Other numerical validations show that the numerical model is able to reproduce the anisotropy of the skin, its heterogeneity and its damage up to failure.
In conclusion, our model of planar and fibrous soft tissues, based on a structural approach, reproduces well the real hyper elastic behavior and the damage mechanisms of the skin. A next step will be the definition of an optimization method for the identification of the model parameters by comparing numerical and experimental results.

FIBROUS TISSUES, FINITE ELEMENT METHOD, FAILURE

IN THE FIELD of transport research, finite element models of the human body are used for the injury risk prediction. The development of these models needs an in-depth knowledge of the mechanical behavior of biological tissue under dynamic loadings up to failure. Unfortunately, comprehensive biomechanical data are missing especially on soft tissues. If we consider planar fibrous soft tissues, such as skin or organ capsules, most experimental studies present quasi static tensile tests inducing small strains and no damage (Lanir *et al.* 1974, Billiar *et al.*, 2000). The objective of this study is to characterize and to model the damage of planar and fibrous soft tissues at high strain rate.

As a first step, we choose to study the skin. This tissue shows 3 layers and only the mean one (the dermis) plays a mechanical role in tension. The dermis is made of a heterogeneous network of collagen and elastic fibers embedded in a ground matrix. The heterogeneity of the tissue needs to perform local measurements and also to include fibers properties in the modeling of its tensile behavior.

In this paper, we first present the experimental characterization of the human skin by using a dynamic tensile test with full strain field measurements. Then in a simulation phase, the skin is modeled by a collagen fibers network. This network is defined by an angular distribution of fibers as the one proposed by Billiar and Sacks (2000) and extended to the damage phase.

MATERIAL AND METHODS

DYNAMIC TENSILE TESTS:

Tensile tests are performed on human skin samples. I-shaped samples are taken off from the forehead of fresh PMHS and kept in a saline solution at 4°C before testing (during 12hours maximum). Samples are cut along 2 perpendicular directions: the transverse direction (noted Tr) which is parallel to the brow line and the cranio-caudal direction (noted Cc).

Prior to test, the skin samples are covered by a random pattern of black dots in order to use the image correlation method (described below) for the strain field measurements.

The dynamic tensile set-up has been described in Jacquemoud et al. (2006) (Figure 1). The system is adapted to an existing vertical drop bay and is composed of 2 trolleys, the main one and the secondary one. Each trolley supports a grip and both are linked together by the tested sample. During the test, the main trolley is stopped by a honeycomb structure and the secondary one pursues its falls, loading the sample. The mass of the secondary trolley is defined as M_0=1.49kg but can be adjusted. Tests are performed at an initial velocity of V_0=3m/s up to failure. The measured strain rates are in the order of 40 s^{-1}.

The set-up is equipped with a load cell, a displacement transducer and a high speed video camera (2000 frames/second). The global longitudinal strain of the sample is computed from the displacement transducer measurements and the full strain field is measured by the image correlation method (Mguil–Touchal *et al.*, 1998) applied to the high speed frames.

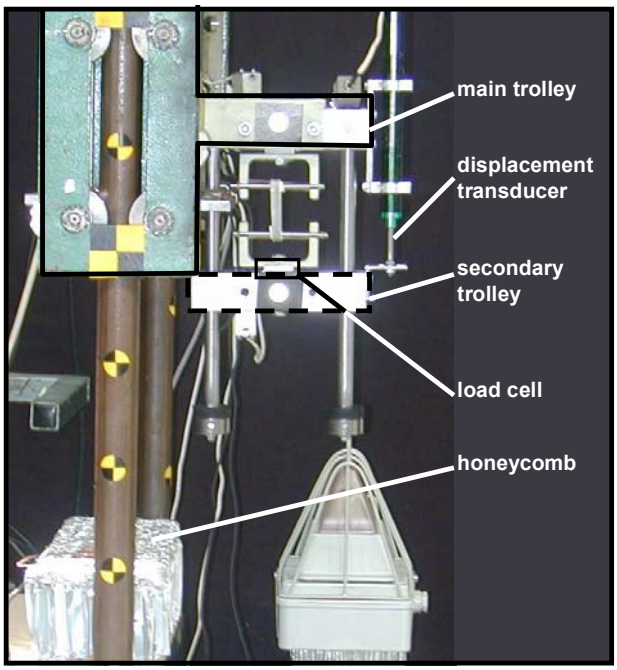

Fig. 1 – Tensile device for dynamic tests on planar soft tissues (presented with a silicone sample)

FINITE ELEMENT MODELING:

The skin is considered as an incompressible membrane with a density of 1. It is modeled by a network of incompressible fibers submitted to plane stress. The skin constitutive law is first written at the fiber scale and then generalized to the membrane scale by integration.

Each fiber behavior is defined from a strain energy potential w_f following the Demiray law (Demiray, 1976). A hydrostatic pressure is included in [1], in order to take into account the incompressibility of the fiber:

$$w_f = a(\exp[b(I_{f1} - 3)] - 1) - \frac{1}{2} p \ln(I_{f3}), \qquad [1]$$

with I_{f1} first invariant of the fiber strains,

I_{f3} third invariant of the fiber strains,
a et b fiber parameters.

The Piola-Kirchhoff stress tensor of each fiber derives from its strain energy potential:

$$\mathbf{S}_f = 2\frac{\partial w_f}{\partial \mathbf{C}_f} \ , \qquad [2]$$

with $\mathbf{C}_f$ is the Right Cauchy-Green strain tensor.

The $\mathbf{S}_f$ tensor is reduced to the S_{f11} component as the fiber is submitted to uniaxial tension. In order to allow the modeling of the fiber failure, S_{f11} becomes:

$$\begin{cases} S_{f11} = 2a.b.\exp\left[b(I_{f1}-3)\right]\left(1-(C_{f11}{}^{-\frac{3}{2}}\right) & \text{si } C_{f11} < C_{11critique} \\ S_{f11} = -0.005C_{f11} + \mathrm{S}_0 & \text{si } C_{11critique} \le C_{f11} < C_{11rupture} \\ S_{f11} = 0 & \text{si } C_{f11} \ge C_{11rupture} \end{cases} \text{, with } \mathrm{S}_0 \text{ constant.} \qquad [3]$$

The fiber organisation in the network is defined by an angular distribution function R proposed by Billiar and Sacks (2000):

$$R(\theta) = \frac{1}{\sigma_R.\sqrt{2\pi}}.\exp\left[\frac{-(\theta-\mu_R)^2}{2\sigma_R{}^2}\right], \qquad [4]$$

with μ_R and σ_R respectively the mean and the standard deviation of the angular distribution

The total strain energy of the membrane W is the sum of fiber strain energies, which depend on their orientations [5]. The Piola-Kirchhoff II stresses of the membrane derive from this energy.

$$W = \frac{1}{Q_0}.\int_{\frac{-\pi}{2}}^{\frac{\pi}{2}} w_f.R(\theta).d\theta \quad \text{with} \quad Q_0 = \int_{\frac{-\pi}{2}}^{\frac{\pi}{2}} R(\theta).d\theta \text{ the initial fiber amount.} \qquad [5]$$

The equilibrium equations are solved using the finite element method with an implicit iterative scheme. Geometrical non linearity is taken into account by using an updated lagrangian formulation applied to isoparametric quadrilateral elements with 4 nodes. The tangent stiffness matrix is computed from the tangent modulus ${}_t\mathbf{A}$ written in the updated lagrangian formulation. Thus, ${}_t\mathbf{A}$ is defined as following:

- if all the fibers show $C_{f11} < C_{11rupture}$, the tangent modulus in a total lagrangian formulation derives from the strain energy potential and is then transformed for the updated lagrangian formulation,
- as soon as a fiber reaches $C_{11rupture}$, the tangent modulus written in the updated lagrangian formulation is directly calculated by finite differences between the researched state and the converged one.

Then, equilibrium equations are solved by an arc length method.

RESULTS AND DISCUSSION

Tensile tests performed on 6 samples taken off in the transverse direction give the following failure characteristics: the ultimate tensile stress = 7.0±1.4MPa (mean ± standard deviation, n = 6) for a local longitudinal strain 19.6±3.5% (mean ± standard deviation, n = 6). The ultimate stress values are similar to those reported by Yamada (1970) and Dunn *et al.* (1983) ranged between 4.6MPa and 14MPa for human skin. The skin seems stiffer in the transverse direction than in the cranio-caudal direction (Figure 2, exp-Tr & exp-Cc). The strain fields measured by image correlation method show the heterogeneity of the tissue. Local high strains are recorded in the failure areas (Figure 3.a).

As a first step of validation, the numerical model is used with 1 element (30x10x1mm^3). Parameters a=0.0150, b=8.8319, $C_{11critique}$=1.45 and $C_{11rupture}$=1.72 are identified on a

representative experimental curve obtained for the human forehead skin in the transverse direction.

The mean μ_R=π/2 and the standard deviation σ_R=π/2 are chosen so that the main direction of the fibers is parallel to the tensile direction, which corresponds to a test in the transverse direction. The curve of longitudinal stress versus longitudinal strain obtained by simulation is close to the experimental values obtained during test #RHD41 performed in the transverse direction (Figure 1, EF-Tr & exp-Tr)

If we define a fiber distribution corresponding to a test in the cranio-caudal direction, i.e. $\mu_R = 0$, the stiffness decreases and the simulated curve is close to the experimental curve obtained for the same subject as the one used for the test #RHD41 but tested in the cranio-caudal direction (test #RHD44) (Figure 1, EF-Cc & exp-Cc).

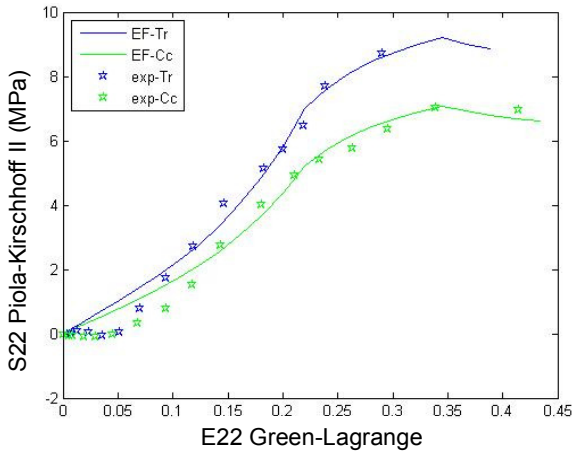

Fig. 2 – Longitudinal stress-strain curves. Experimental values for transverse tensile direction (exp-Tr) and cranio-caudal tensile direction (exp-Cc).
Finite element simulation (1 element) with μ_R =π/2 (EF-Tr) and μ_R =0 (EF-Cc).

The second step of the model validation is performed using a sample of the same size as in the first step (30x10x1mm^3) but made of 48 elements. All the parameters are the same as in the first step, except μ_R . The values of μ_R are randomly defined between -π/2 and π/2, on each element (Figure 3.b) so that the simulated structure is heterogeneous. In this case, it appears that the strain field becomes heterogeneous before the failure occurrence (Figure 3.c).

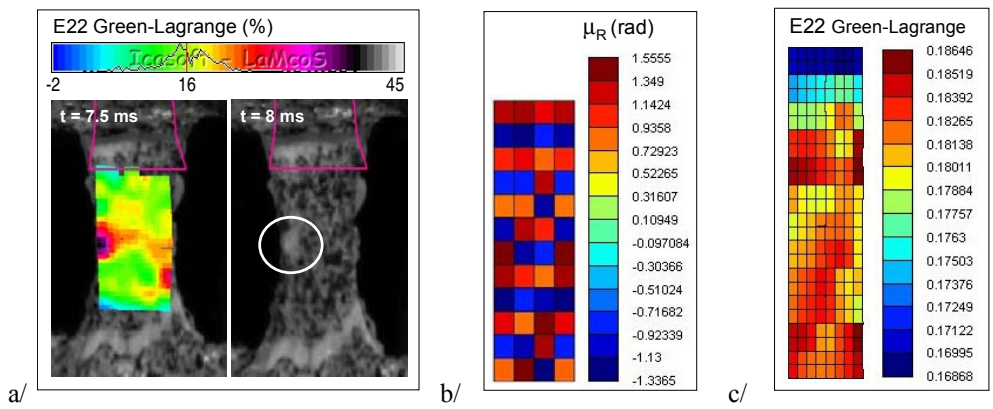

Fig. 3 – a) Longitudinal strains measured by the image correlation method (test #RHD14),
(b) Fiber angular distribution on the FE model at t = 0 ms (48 elements),
(c) Longitudinal strains simulated with FE model (48 elements).

CONCLUSIONS

Tensile test protocol adapted to planar soft tissues has been carried out on human skin samples. The use of the image correlation method allows obtaining local strains in the area of the failure and gives the 3 components of the strain field, with a unidirectional test. Moreover this method is without contact and thus avoids any risk of tissue damage.

The experimental results obtained showed the anisotropy of the forehead human skin which is linked to the fiber main directions. Moreover, the measured strain field is heterogeneous, which well reflects the structural heterogeneity of the tissue. The use of uniaxial tensile loading on isolated skin sample does not correspond to a realistic in vivo loading of this tissue. Yet, the induced strain field is fully recorded by the image correlation method and the test gives the required data for the 2D model validation.

From these experimental results, a finite element model has been developed to simulate the behavior of a heterogeneous fibrous network up to failure. The hyper elastic brittle model used seems to be able to describe the skin behavior up to failure.

A next step of the numerical developments will be the definition of an optimization method to improve the identification of the parameters used in our model by comparing numerical and experimental results.

References

Demiray, H., Stresses in ventricular wall. *ASME J. Appl. Mech.,* 43, 1976, 194-197.

Dunn, M.G., Silver, F.H., Viscoelastic behavior of human connective tissues: relative contribution of viscous and elastic components. *Connect. Tissue Res*., 12, 1983, 59-70.

Jacquemoud, C., Bruyère-Garnier, K., Coret, M., Methodology to determine failure characteristics of planar soft tissues using a dynamic tensile test. *Journal of Biomechanics.* **40**(2), 2007, 468-475.

Lanir, Y., Fung, Y.C., Two-dimentional mechanical properties of rabbit skin - II. Experimental results. *Journal of Biomechanics.* **7**, 1974, 171-182.

Mguil - Touchal, S., Morestin, F., Brunet, M. Experimental determination of forming limit diagrams using a method of digital picture. In proceedings of the 20th Biennal Congress. Genval Brussel, IDDRG 98, 1998, Brussel.

Billiar K.L., Sacks M.S., Biaxial mechanical properties of the natural and glutaraldehyde treated aortic valve cusp Part II: A structural constitutive model, Journal of Biomechanical Engineering, **122**(4), 2000, 327-335.

Yamada, H., Mechanical properties of the nervous system, integument, sense organs and tissues. In: Evans, G. (Ed.), Strength of biological materials. Waverly Press, Baltimore, 1970, 224-231.